Macromolecules
Article
pubs.acs.org/Macromolecules

New Approach for Analyzing the Vertical Structure of Polymer Thin Films Based on Surface-Enhanced Raman Scattering

Sivan Linde, Antonio Carella, and Rafi Shikler*

Department of Electrical and Computer Engineering, Ben-Gurion University of the Negev, Beer-Sheva 84105 Israel

Ⓢ *Supporting Information*

ABSTRACT: We report on a new approach for measuring the chemical composition of the 20 nanometers at the top or bottom of a polymer film. This approach is based on a variation of the surface enhanced Raman scattering effect with laser illumination through a thin gold layer (~4 nm). We show that the introduction of the thin gold layer has little or no effect on the morphology of the film that is spin coated on top of it. We demonstrate that this technique has better than 20 nanometer vertical resolution by studying bilayers of polyfluorines with varying thicknesses and by showing the existence of top and bottom wetting layers in a polymer blend of the same polymers. We also show that the top wetting layer is thinner than the bottom one. The difference in thicknesses explains how a solar cell with an electron blocking layer at the cathode works.

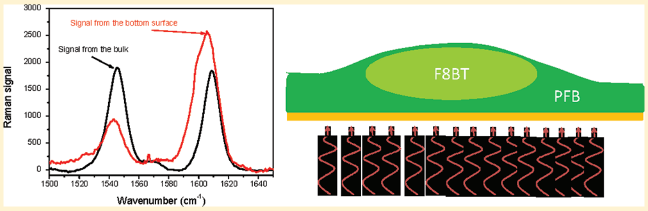

■ INTRODUCTION

In recent years, organic optoelectronic devices based on polymers and small molecules are becoming more and more popular, ranging from organic light emitting diodes (OLED)[1−7] through organic solar cells,[8−11] organic thin film transistors (OTFT)[12,13] and more. The attractive properties of these devices that make them so popular are large versatility of the optoelectronic properties of the materials, ease of manufacturing, excellent mechanical properties and ultrathin thickness. A commonly used architecture in many devices, such as OLED and organic photovoltaic (OPV), is vertical and hence, their functionality is largely determined by the chemical structure and composition in the vertical direction. For the study of the influence of the chemical structure and composition on the optoelectronic properties, characterization techniques with better than 50 nm vertical resolution need to be developed, because the common thicknesses of these devices is around a hundred nanometer

Analysis of the vertical structure is usually performed by using either environmental scanning electron microscopy (ESEM) on a cleaved sample[14] or X-ray photoelectron spectroscopy (XPS).[15] The drawbacks of these two techniques are that they are destructive in nature and therefore, cannot be applied in situ to a working device and they both lack spatial resolution in the horizontal direction. A method that has high spatial resolution in all three directions is nanotomography.[16] This technique gives three-dimensional images with high spatial resolution of the topography of the films. However, this technique cannot give an indication on the chemical composition, unless a specific topography feature can be associated with a specific chemical structure. Moreover, because it is based on transmission electron microscope (TEM) it cannot be applied to working devices. A different approach that is short-range and sensitive to the chemical composition is the surface enhanced Raman scattering technique (SERS). The SERS effect[17−23] is a variant of the Raman effect where the Raman cross-section is considerably enhanced in the presence of plasmons in metals. The SERS effect is used to detect low quantities of materials, to study materials that have low Raman cross-section or to study the interaction between a substrate and a thin layer of metal that is gradually deposited on it. Traditionally, there are two commonly used configurations for studying materials with low Raman cross-section. In the first, a periodic structure of gold (Au) or silver (Ag) is evaporated on an opaque sample. In the second, nanoparticles (~15−20 nm in size) of the same metals are deposited on a similar substrate. In both cases, the plasmons in the metal enhance the Raman cross section by up to 7 orders of magnitude.[17−19] However, the size of the nanoparticles and the characteristics length of the periodic structure are large compared to the typical thickness of the films we aim to study and can therefore, affect their morphology. Therefore, these configurations are unsuitable for studying the morphology of thin films.

A different SERS technique is used when the aim of the study is to investigate the interaction between organic materials and metals that are evaporated on top of them as reported by Paez et al.[24,25] and by Davis and Pemberton.[26,27] In these studies, a thin layer of metal was evaporated on top of the organic layer while monitoring changes in the Raman spectra as a function of the evaporated material and its thickness. One of the findings of these studies is that when the evaporated metal is gold or silver (noble metals) and they do not chemically interact with the material the only observed effect is the enhance the Raman signal. Moreover, due to the short-range of the SERS effect, the

Received: August 17, 2011
Revised: January 20, 2012
Published: February 1, 2012

dx.doi.org/10.1021/ma201867e | *Macromolecules* 2012, 45, 1476−1482

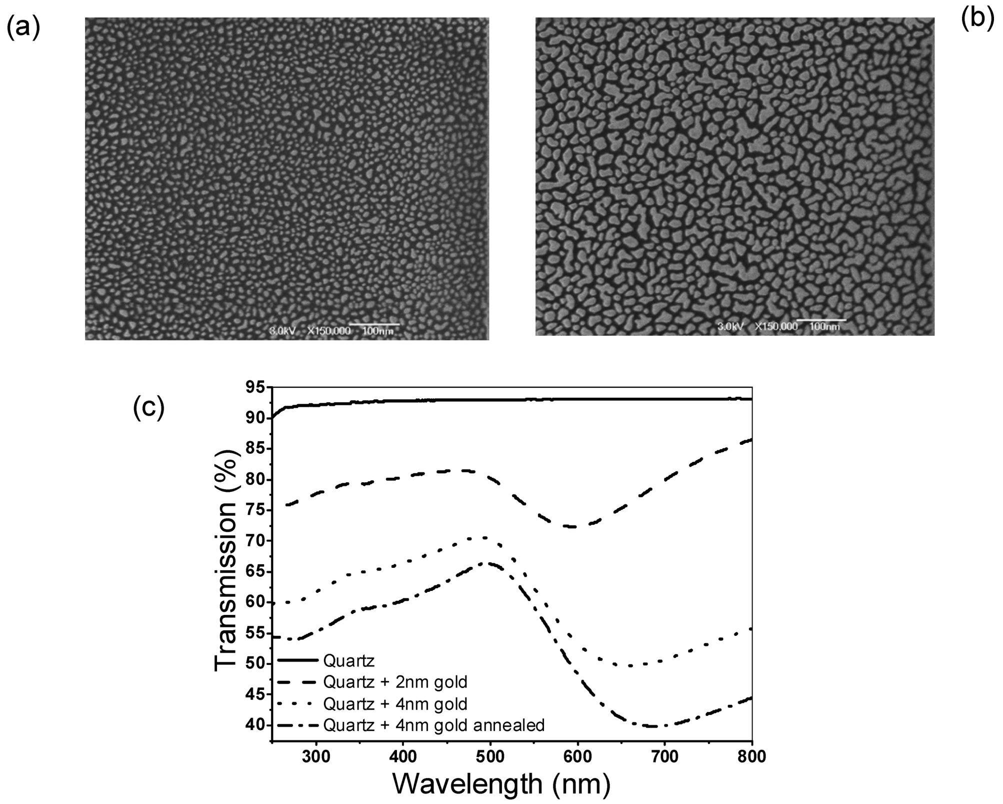

Figure 1. SEM images of 2 nm (a) and 4 nm (b) of thermally evaporated gold on silicon. UV–vis measurements of these layers on quartz substrates.

enhanced Raman signal will only come from the material that is close to the evaporated metal. This combination, of no chemical reaction and short-range interaction, is the motivation behind our idea to study the vertical chemical composition of organic structures using thermally evaporated thin layer of gold (thickness ≤4 nm) on a transparent substrate and illuminate through it using SERS technique.

■ EXPERIMENTAL SECTION

In all the experiments reported here we used two polyfluorenes polymers, a hole conductor Poly[(9,9-dioctylfluorenyl-2,7-diyl)-*co*-(*N*,*N*′-diphenyl)-*N*,*N*′-di(*p*-butylphenyl)-1,4-diaminobenzene)] (PFB) and an electron conductor poly[(9,9-dioctylfluorenyl-2,7-diyl)-*alt*-co-(1,4-benzo{2,1′,3}thiadiazole)] (F8BT) (American Dye Company). We chose these polymers because they have large Raman cross-section and because bilayer and blend structures made from these materials are extensively reported in the literature.[28,29,14,15] The polymers were spin-casted from a 1.5% (by weight) *p*-xylene solution. PEDOT:PSS (Clevios) was purchased from H. C. Starrck and was filtered using 0.45 μm PVDF filter. We used quartz slides that were precleaned in an ultra sonic bath using acetone, methanol and iso-propanol as substrates. The cleaning process was followed by exposure to oxygen plasma for 5 min. The cleaned substrates were then partially covered with 4 nm of gold, evaporated at 10^{-7} Torr and at a rate of 0.1 nm/s through a shadow mask. The bilayer structures were fabricated using water-floating technique to float the F8BT films that were separately prepared on a glass substrate as outlined by Xia.[30] All the Raman and topographic measurements were done on a unique set up the combines the NANOWIZARD 2 atomic force microscope (JPK GMBH) for thickness and topography measurements and iHR550 spectrograph (Horiba Jobin Yvon) for Raman measurements with laser source at 660 nm. This unique setup allows separate measurements of AFM and Raman. It also allows micro-Raman measurements using the AFM to accurately position the Raman laser at specific points across the sample. This unique combination enables us to correlate topography and Raman measurements with around 1 μm spatial resolution (defined by the numerical aperture of the lens). We used Jasco V-750 spectrophometer for UV–vis measurements.

■ RESULTS AND DISCUSSION

The proposed technique is based on the evaporation of a thin layer of gold (thickness ≤4 nm) on a transparent substrate and illuminates through it for SERS measurements. To this end we studied two thicknesses of gold layer, 2 and 4 nm. The SEM images of these layers along with their absorption curves are shown in Figure 1. We could not measure the film thickness directly because as seen in Figure 1, parts a and b, the film is discontinuous and therefore the reported thickness is the one measured using the evaporator thickness monitor.

We can see in Figure 1c that at the thickness of 4 nm the absorption of the gold is maximized around 660 nm (the Raman laser wavelength). This implies that the enhancement due to SERS is maximized at a thickness of 4 nm. It is also shown that upon annealing, the plasmons resonance and hence the maximum absorbance is red-shifted to 700 nm. This implies that the coupling to the surface plasmons of the gold and therefore the resulting SERS effect decrease upon annealing.

For practical and future use of this technique for the study of working organic optoelectronic devices, it is important that the thin gold layer will have minimum effect on device performance. As shown in Figure 1, parts b and c, because the gold layer is discontinuous, it has a transparency larger than 60% for wavelengths smaller than 500 nm, the wavelength region where optoelctronic devices made from these polymers absorb and emit light.[28,31] In addition, the work function of gold ~5.0 eV[32] is similar to the work function of ITO after oxygen plasma treatment,[28] and thus it should have small effect on the

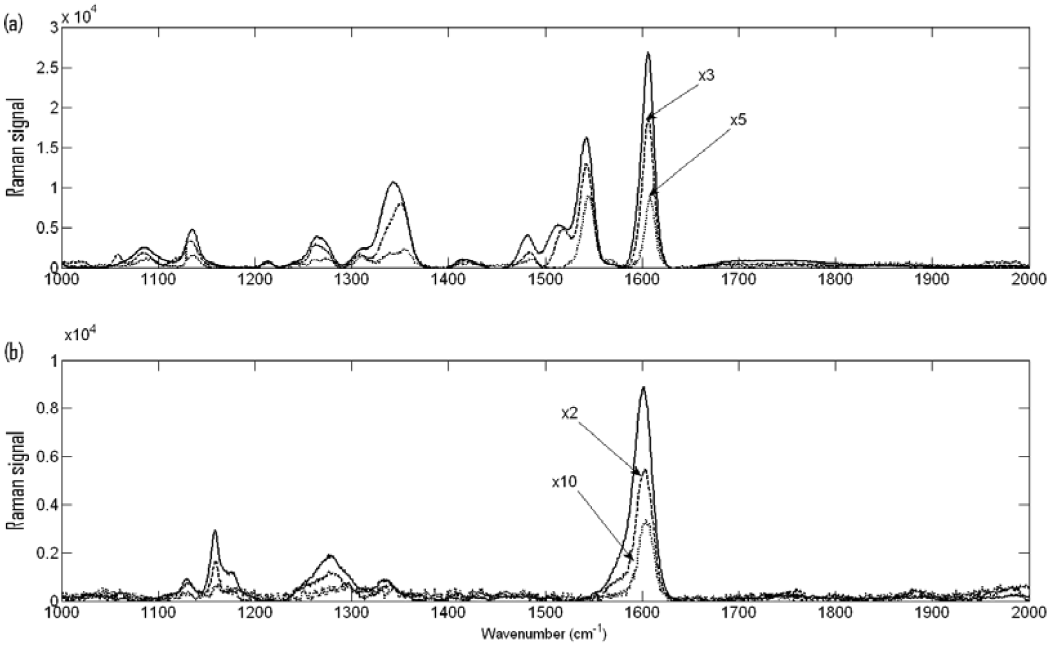

Figure 2. Raman spectra of F8BT (a) and PFB (b) under 660 nm laser. The dotted line is taken on the bare quartz, the dashed line is taken on 4 nm of gold annealed overnight, and the solid line is taken on 4 nm gold without annealing.

electrical properties of the contacts when measuring working optoelectronic devices.

We can also control the layer surface tension by varying the time between the evaporation and film deposition and therefore control the wetting properties of the gold. Through evaporation and up to 5 min the gold surface remains hydrophilic while over longer periods it becomes hydrophobic.[33]

The first step was studying the Raman spectra of the homopolymers and understands the effect of the interfacial thin gold layer. Raman spectra of 80 nm F8BT and PFB films in the region between 1000 and 2000 cm^{-1}, the region where the highest Raman peaks appear are shown in Figure 2, parts a and b, respectively.

Parts a and b of Figure 2 show three Raman spectra taken on bare quartz (dotted line), on overnight annealed (in a vacuum oven at 120 °C) polymer film on 4 nm gold layer (dashed line) and on as evaporated 4 nm gold layer (solid line). We also measured the Raman spectra of the polymer films after casting them on an annealed gold layer but without annealing the polymer film and found the results very similar to those of the annealed films (dashed line). For both homopolymers, the Raman spectra taken over the gold (with and without annealing) is enhanced in respect to the one taken on the bare quartz. As can be seen the Raman signal is smaller for the annealed samples. We assume that this change probably occurs due to the reduction in the laser-plasmon coupling as seen by the red shift in the plasmons resonance in Figure 1c. We cannot test whether or not the gold diffuses into the polymer layer but we assume that this diffusion (if exists) does not affect the chemical properties of the structure. Because the spectra of the films that were annealed with the thin gold layer and those that were casted on an annealed gold layer but were not annealed were the same. We present the measurement of the annealed sample as a basis for the next measurements in which we study the Raman spectra of a bilayer structure and the baking procedure is an inherent part of the fabrication procedure.

In Figure 2a of the Raman spectra of the F8BT, two distinguished peaks appear at ~1546 and ~1609 cm^{-1}.[27,28,15] The enhancement due to the SERS effect is more pronounced in the 1609 cm^{-1} peak in comparison with 1546 cm^{-1}. The ratio between these two peaks is about 0.9 when the measurement is performed on the bare quartz while it increases to about 1.5 on the gold covered area of the substrates. This is due to the different coupling strengths of the gold plasmons to the different Raman modes. Moreover, it can be seen that for the F8BT there is an additional peak that appears (~1520 cm^{-1}) when the spectrum is taken on gold. The new peak is an IR mode that becomes active in the presence of the metal.[23,24] The second polymer, PFB, has only one peak in this region ~1603 cm^{-1}.[15,27]

After studying the fingerprints of the SERS effect on each polymer we studied two structures that are common for organic photovoltaic devices made from polymers, namely bilayer and blend structure of F8BT and PFB. The bilayer structure provides us with vertical control on the thickness of the two homopolymer layers separately, and hence, enables us to test the vertical resolution of our technique. The blend structure cannot be controlled but previous studies by Kim et al. and us show the existence of wetting layers of PFB both on the glass and at the air interface and that the thickness of the wetting layers is in the range of 10 to 15 nm.[34,15] The existence of a PFB layer at the anode interface is beneficial as PFB is a hole conductor. The existence of the PFB at the cathode interface can degrade the device performance as PFB blocks the electrons from reaching the cathode. However, devices made from these blends work as solar cells, therefore it is assumed that the thickness of the PFB layer close to the cathode must be small but this assumption has not been proven yet.

The bilayer structures we have studied have the following architecture: thin film of constant thickness (85 ± 5 nm) of F8BT on top of a thin film with varying thicknesses (60, 50, 20 ± 5 nm) of PFB. The different thicknesses of the PFB films were obtained by controlling the spin coater spinning velocity.

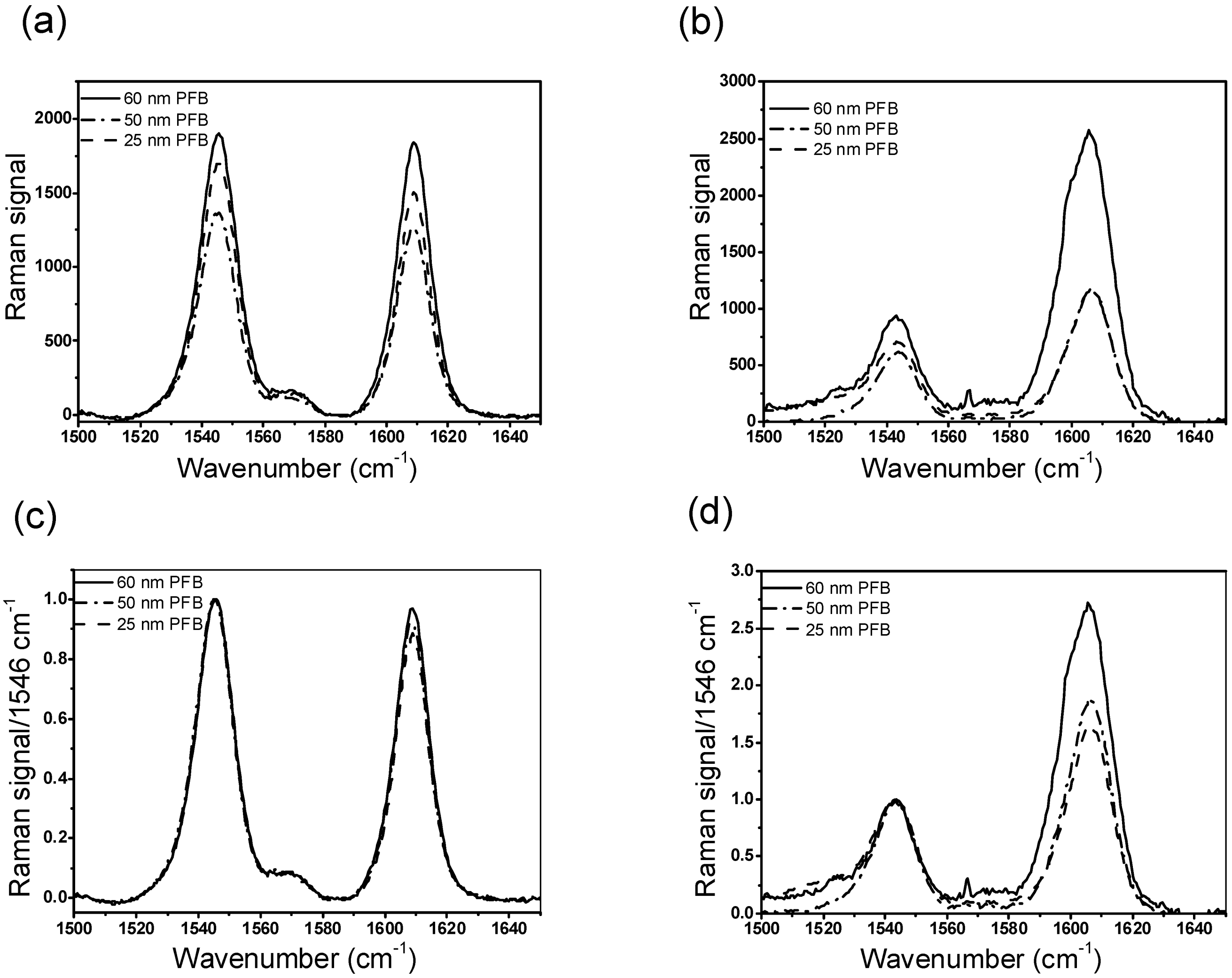

Figure 3. Raman spectra of a bilayer with different thicknesses of PFB, 60 nm 50 and 25 nm for the straight, dashed and dotted line, respectively. Spectra taken outside the gold coated area as measured (a) and normalized to by the 1546 cm^{-1} peak (c). Spectra taken on 4 nm of gold as measured (b) and normalized by the 1546 cm^{-1} peak (d).

The thicknesses of the F8BT and PFB films were measured using an atomic force microscope. We chose a constant thickness for the F8BT as we wanted the Raman signal that originates from to F8BT to be same for all samples.

Parts a and b of Figure 3 show Raman spectra measurements of the bilayers with different thicknesses of PFB films over bare quartz and over gold-coated quartz, respectively. Because the F8BT thickness is the same we have normalized the results by dividing the Raman spectrum by the height of the peak at 1546 cm^{-1} for both the bare and gold coated areas, Figure 3, parts b and d, respectively.

By comparing the spectra taken outside the gold coated area to the spectra taken on the gold area we can see that the for the same film the height of the peak which is only associated with the F8BT, i.e. the 1546 cm^{-1} peak, is smaller on the gold coated substrate compare to the uncoated areas. This complies with the fact that the intensity of the light reaching the F8BT layer should be lower after passing through the absorbing gold layer and hence should results in lower amplitude. The F8BT signal is not affected by the SERS effect as it is rather far from the gold layer. However, we do see a slight increase in the left-hand side of the 1546 cm^{-1} peak for the 25 nm thick sample, which might indicate the start of a shoulder as seen for pure F8BT samples (Figure 2a). In contrast, the ~1609 cm^{-1} peak which is common to both materials is largely enhanced on gold coated areas as expected based the larger enhancement seen for the PFB on gold sample (Figure 2b). We observe that in the measured spectra there is no direct relation between the PFB film thickness and the height of the Raman peaks. The reason is that the height of the peaks do not only dependent on the volume of the materials, i.e., the thickness of each polymer layer, but also on the magnitude of the electric field at this layer. This cannot be easily calculated as we have only a rough estimate of the thicknesses of the layers and the interface between them and we do not know the effect of gold diffusion on the optical properties of the entire structure. We then normalized the Raman spectra by the height of the 1546 cm^{-1} peak. The normalization is motivated by the constant thickness of the F8BT film. The normalized spectra are shown in Figure 3, parts c and d, for the bare and gold coated areas, respectively.

In the normalized Raman measurements taken on bare quartz, the relative height of the peak around ~1609 cm^{-1} goes down slightly with the reduction of the thickness of the PFB layer and is always smaller than one (Figure 3c). This is because the PFB Raman cross-section is twice as small as the F8BT, and Raman signal is roughly proportional to the volume of the

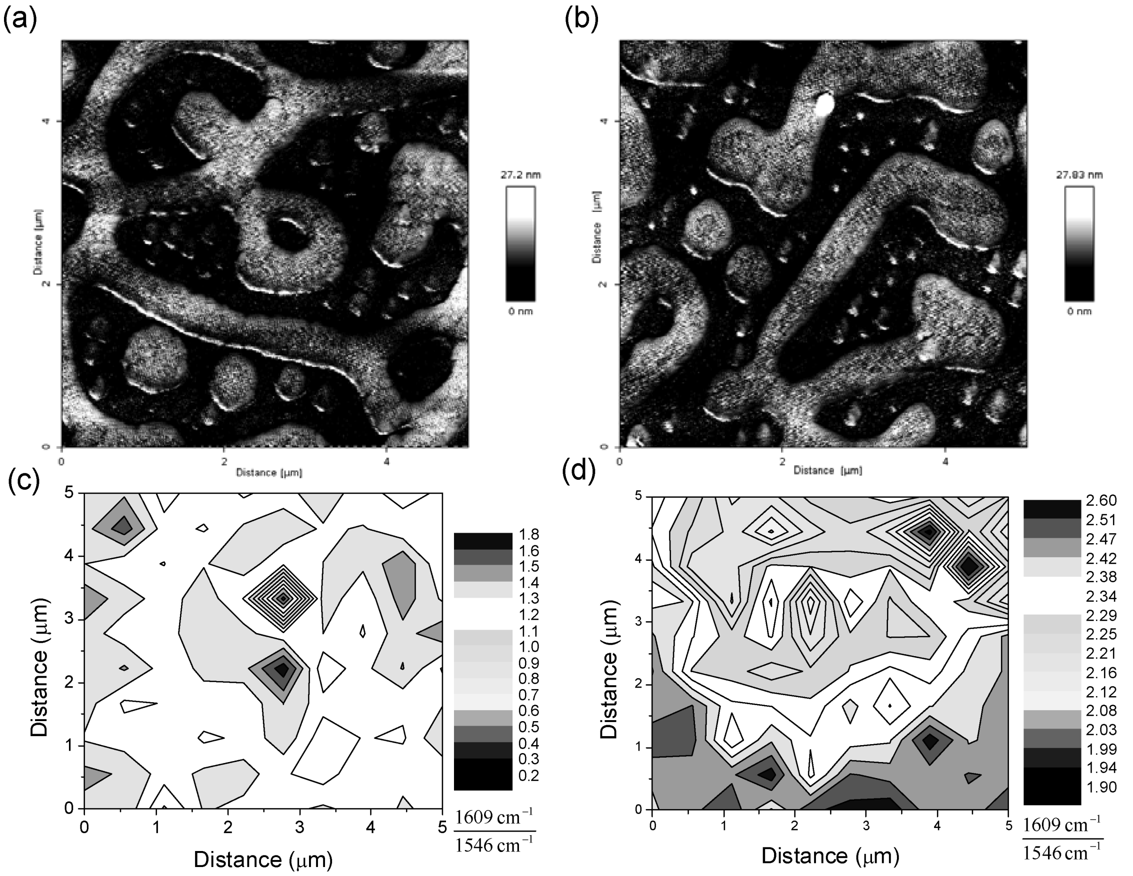

Figure 4. AFM maps of 1:1 PFB and F8BT blend on bare quartz (a) and on 4 nm gold coated quartz (b). A map of the ratio between the ~1609 cm^{-1} and the 1546 cm^{-1} peaks in the coated and bare samples (c and d), respectively.

layer.[15,30] This changes when we look at the normalized Raman spectra that were taken on the gold coated areas (Figure 3d). In this case, the peak around 1605−1609 cm^{-1} is always higher than the 1546 cm^{-1} peak (up to three times higher). A ratio larger than one was also observed for the pure F8BT structure. However, the ratio between the 1609 and 1546 cm^{-1} peaks or a pure F8BT sample in Figure 2a is less than 1.5 for the annealed sample while even for the 25 nm thick PFB sample this ratio is 1.65. This is clear evidence that the dominant part of the 1609 cm^{-1} signal comes from the PFB. This can only happen if the PFB signal is enhanced by the SERS effect because as mentioned above the Raman cross-section of PFB is smaller than F8BT

A closer inspection of the positions of the ~1609 cm^{-1} peaks for the 4 nm gold coated sample Figure 3d, shows that it moves from 1605 to 1607 cm^{-1} as the thickness of the PFB layer is reduced from 60 to 25 nm. This is an additional indication to the enhancement of the PFB signal as its peak is at 1603 cm^{-1} compared to the 1609 cm^{-1} of the F8BT. When an inverted structure with PFB on top of F8BT was measured, the measured spectrum resembled the dashed line of Figure 2a. The larger ratio between the heights of the ~1609 and 1546 cm^{-1} peaks and the lack of the shoulder at 1520 are direct evidence that our technique vertical discrimination is better than 25 nm, the smallest PFB thickness.

In the next step we have studied a 1:1 blend of F8BT and PFB. Similar blends were studied before and it was verified that the PFB wets the substrate and the air interface.[15] However, due to lack of vertical sensitivity, the thickness of the PFB has only estimated to be around 15 nm based on the testing instrument specification. We spin coated the blend on a 4 nm gold coated quartz substrate and on a bare quartz substrate. We measured the topography of the blends using atomic force microscope (AFM) as can be seen in Figure 4 (a) and (b) for the gold coated and bare areas of the substrate, respectively.

In parts a and b of Figure 4, the higher areas (the brighter colors) are the F8BT-rich phases and the lower areas are the PFB-rich phases. These two sub figures show that the thin gold layer have little or no effect on the blend morphology as shown by the similar topographic features. We used the system described above that combines an AFM and Raman for the scanning Raman measurements and took a hundred spectra over the area scanned by the AFM. The measured Raman spectra was normalized in the same manner as in the bilayer measurements to show the ratio of the 1609 and 1546 cm^{-1} peaks on the bare quartz and on the gold coated quartz are shown in Figure 4, parts c and d, respectively. Because the measured film is a blend rather than a bilayer, the value of the ratio of these peaks for the bare quartz sample indicates the relative composition of the two blend components at the measured point. The higher the ratio, the lower is the amount of F8BT at the measured point. It can be seen that there are few areas that are almost pure F8BT (ratio ~ 0.9) and there are other places when it is around 40% of F8BT (ratio ~ 1.4). However, the picture is different for similar spectra taken on the gold-coated area of the substrate (Figure 4d). In Figure 4d, we see that the minimum value of the ratio between the peaks is over 2. As we show above, for a pure F8BT sample this ratio is limited to 1.5. This is a first indication to the presence of PFB wetting layer at the gold layer. This is further supported by

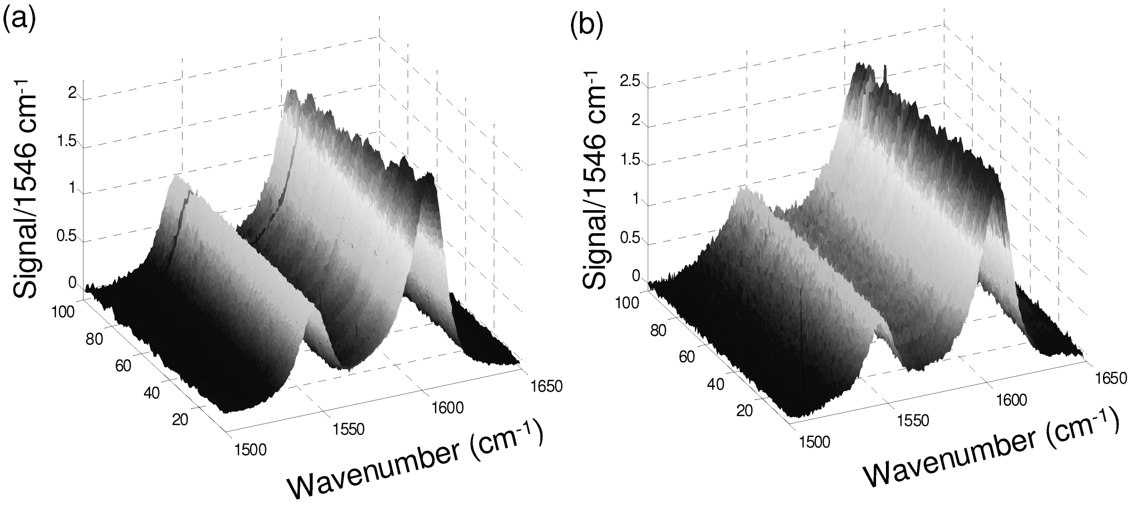

Figure 5. Combined hundred Raman spectra of an F8BT:PFB blend taken over an a region of 5 μm × 5 μm with 4 nm gold coating on top (a) and on for the same blend shown in Figure 4d.

studying what is missing from the spectra. Figure 5b shows a plot of all the normalized spectra taken at each point of the map in Figure 4d. We see that the shoulder around 1520 cm^{-1}, which appears when the F8BT is in direct contact with the gold layer (Figure 2a), is missing.

Because the effect of the Plasmon enhancement is not directional, a thin gold layer can also be evaporated on top of the structure with similar expected effects. We have repeated the same procedure we have done for coating the quartz with gold and evaporate thin gold layer on top of the films. The results are shown in Figure 5a. It is known from previous works that there are no changes in the film's structure due to the introduction of the film into vacuum.[9,14,15,34] In Figure 5a, the shoulder at 1520 cm^{-1} which is an indication of a F8BT top layer, is again absent. This is in agreement with the results of Kim et al.[15] Because the vertical resolution of the XPS used by Kim et al. was ~15 nm, they estimated that the thicknesses of the wetting layers at the top and bottom of the blend film are similar.[15] However, our results provide additional information. The values of the normalized spectra at ~1609 cm^{-1} are smaller, for the top gold layer, which indicate that the top wetting layer is thinner than bottom one. This explains why the presence of a top PFB wetting layer does not affect the performance of solar cells made from this blend. This result is consistent with the model presented by Chiesa et al.[34]

In many optoelectronic devices based on polymers, PEDOT:PSS is used as an electron blocking layer on the anode.[35] The thickness of this layer is around 40−50 nm, and therefore, if the semitransparent gold layer is deposited directly on the gold it cannot be used to probe the polymer layers above the PEDOT:PSS due to the short distance of the SERS effect. Therefore, we checked how we can use our technique to study polymer films that were deposited on top of the PEDOT:PSS layer. We studied the following architecture consisted of an ITO coated quartz substrate with an additional layer of PEDOT:PSS. On top of the PEDOT:PSS layer we have deposited the 4 nm gold layer. Because PEDOT:PSS is hygroscopic we did not fabricated a bilayer device but studied the Raman spectrum of F8BT that was spin coated directly on the thin gold layer. Figure 6 shows Raman spectra taken on and off the gold coated areas. It is clearly seen that the two normalized spectra are similar to the ones taken on and off the gold on quartz as shown in Figure 2a with similar values for the 1609 cm^{-1} peak. This prove that our technique can by used to probe different zones in the device as long as the electrical characteristics of gold is consistent with those of the layers underneath it.

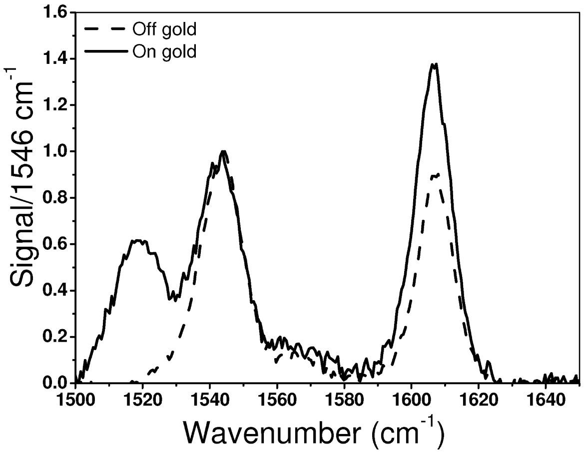

Figure 6. . Raman spectra of an F8BT layer on top of PEDOT:PSS layer with gold between the layers (solid line) and off the gold-coated area (dashed line).

■ CONCLUSIONS

In this paper, we proposed a new method based on SERS effect for the analysis of the bottom and top 20 nm polymer films. This method is based on the evaporation of a thin layer of gold on quartz and ITO-coated quartz slides. We demonstrated the capabilities of this technique by studying bilayer structures of two polyfluorene polymers with varying bottom layer thickness. We have observed that the dominant contribution to the Raman peak around 1609 cm^{-1} comes from the SERS enhancement of the PFB signal even when the thickness of the PFB layer was only 25 nm. We also studied a 1:1 blend of the same polymers using a combination of AFM and scanning Raman and showed the existence of a wetting layer of PFB on the top and bottom of the film. From previous works, we know that the thickness of this wetting layer is around 15 nm. This proves that the vertical resolution of the proposed technique is around 20 nm. Our measurements indicate that the top layer is thinner then the bottom layer. This discovery explains why solar cells made from this blend work even when an electron blocking layer is present on the interface to the cathode. Our work can be extended to degradation studies due to the similar work functions of gold and ITO and the high transparency of the gold coated ITO (better than 65%). We are now in the process of applying this technique to study in situ working organic optoelectronic devices.

■ ASSOCIATED CONTENT

Ⓢ Supporting Information

Absorption spectra of F8BT and PFB on plain quartz an on 4 nm of gold. This material is available free of charge via the Internet at http://pubs.acs.org.

■ AUTHOR INFORMATION

Corresponding Author

*Telephone: 0097286472567. Fax: 0097286472949. E-mail: rshikler@ee.bgu.ac.il.

Notes

The authors declare no competing financial interest.

■ REFERENCES

(1) Burrows, P. E.; Gu, G.; Bulovic, V.; Shen, Z.; Forrest, S. R.; Thompson, M. E. *IEEE Trans. Elec. Dev.* **1997**, *32*, 1188−1203.

(2) Friend, R. H.; Gymer, R. W.; Holmes, A. B.; Burroughes, J. H.; Marks, R. N.; Taliani, C.; Bradley, D. D. C.; Dos Santos, D. A.; Bredas, J. L.; Logdlund, M.; Salaneck, W. R. *Nature* **1999**, *397*, 121−128.

(3) Morgado, J.; Friend, R. H.; Cacialli, F. *Appl. Phys. Lett.* **2002**, *80*, 2436−2438.

(4) Bernius, M. T.; Inbasekaran, M.; O'Brien, J.; Wu, W. S. *Adv. Mater.* **2000**, *12*, 1737−1750.

(5) Wilkinson, C. I.; Lidzey, D. G.; Palilis, L. C.; Fletcher, R. B.; Martin, S. J.; Wang, X. H.; Bradley, D. D. C. *Appl. Phys. Lett.* **2001**, *79*, 171−173.

(6) Lee, K. H.; You, J. N.; Kang, S.; Lee, J. Y.; Kwon, H. J.; Kim, Y. K.; Yoon, S. S. *Thin Solid Films* **2010**, *518*, 6253−6258.

(7) Seo, J. H.; Lee, K. H.; Seo, B. M.; Koo, J. R.; Moon, S. J.; Park, J. K.; Yoon, S. S.; Kim, Y. K. *Org. Elect.* **2010**, *11*, 1605−1612.

(8) Yu, G.; Gao, J.; Hummelen, J. C.; Wudl, F.; Heeger, A. J. *Science* **1995**, *270*, 1789−1791.

(9) Halls, J. J. M.; Walsh, C. A.; Greenham, N. C.; Marsegalia, E. A.; Friend, R. H.; Moratti, S. C.; Holmes, A. B. *N ature* **1995**, *376*, 498−450.

(10) Brabec, C. J.; Sariciftci, N. S.; Hummelen, J. C. *Adv. Funct. Mater* **2001**, *11*, 15−26.

(11) Liang, Y.; Xu, Z.; Xia, J.; Tsai, S. T.; Wu, Y.; Li, G.; Ray, C.; Yu, L. *Adv. Mater.* **2010**, *22*, E135−E138.

(12) Klauk, H. *Chem. Soc. Rev.* **2010**, *39*, 2643−2646.

(13) Zschieschang, U.; Ante, F.; Yamamoto, T.; Takimiya, K.; Kuwabara, H.; Ikeda, M.; Sekitani, T.; Someya, T.; Kern, K.; Klauk, H. *Adv. Mater.* **2010**, *22*, 982−985.

(14) Ramsdale, C. M.; Bache, I. C.; MacKenzie, J. D.; Thomas, D. S.; Arias, A. C.; Donald, A. M.; Friend, R. H.; Grennham, N. C. *Phys. E* **2002**, *14*, 268−271.

(15) Kim, J. S.; Ho, P. K. H.; Murphy, C. E.; Friend, R. H. *Macromolecules* **2004**, *37*, 2861−2871.

(16) Bavel, S. S.; Sourty, E.; de With, G.; Loss, J. *Nano Lett.* **2000**, *9*, 507−513.

(17) Fleischmann, M.; Hendra, P. J.; McQuillan, A. J. *Chem. Phys. Lett.* **1974**, *26*, 163−166.

(18) Moskovits, M. *Rev. Mod. Phys.* **1985**, *57*, 783−826.

(19) Moskovits, M.; Tay, L. L.; Yang, J.; Haslett, T. *Opt. Prop. Nanostruct. Random Media* **2002**, *82*, 215−226.

(20) Aroca, R. *Surface enhanced vibrational spectroscopy*. Wiley: New York, 2006.

(21) Persson, B. N. J.; Zhao, K.; Zhang, Z. Y. *Phys. Rev. Lett.* **2006**, *96*, 207401−207404.

(22) Kneipp, K.; Wang, Y.; Kneipp, H.; Perelman, L. T.; Itzkan, I.; Dasari, R.; Feld, M. S. *Phys. Rev. Lett.* **1997**, *78*, 1667−1670.

(23) Otto, A. *Phys. Status Solidi A* **2001**, *188*, 1455−1470.

(24) Paez, B. A.; Salvan, G.; Scholz, R.; Zahn, D. R. T. *Phys. Status Solidi C* **2005**, *2*, 4048−4052.

(25) Zahn, D. R. T.; Salvan, G.; Gavrila, G.; Paez, B. A.; Kramer, B. *Adv. Solid State Phys.* **2006**, *45*, 313.

(26) Davis, R. J.; Pemberton, J. E. *J. Phys. Chem. C* **2008**, *112*, 4364−4371.

(27) Davis, R. J.; Pemberton, J. E. *J. Phys. Chem. C* **2009**, *112*, 4397−4402.

(28) Ariu, M.; Lidzey, D. G.; Bradley, D. D. C. *Synth. Met.* **2000**, *111*, 607−610.

(29) Kim, J. S.; Ho, P. K. H.; Murphy, C. E.; Baynes, N.; Friend, R. H. *Adv. Mater.* **2002**, *14*, 206−209.

(30) Xia, Y.; Friend, R. H. *Appl. Phys. Lett.* **2006**, *88*, 163508−163511.

(31) Shikler, R.; Chiesa, M.; Friend, R. H. *Macromolecules* **2006**, *39*, 5393−5399.

(32) Dimitrakopoulos, C. D.; Malenfant, P. R. L. *Adv. Mater.* **2002**, *14*, 99−117.

(33) Smith, T. J. *Colloid Interface. Sci.* **1980**, *75*, 51−55.

(34) Chiesa, M.; Bürgi, L.; Kim, J. S.; Shikler, R.; Friend, R. H.; Sirringhaus, H. *Nano Lett.* **2005**, *5*, 559−563.

(35) Roman, L. S.; Mammo, W.; Petersson, L. A. A.; Andersson, M. R.; Inganas, O. *Adv. Mater.* **1998**, *10*, 774−777.